International Journal of Thermophysics, Vol. 14, No. 5, 1993

Measurement of Surface Tension of Tantalum by a Dynamic Technique in a Microgravity Environment

A. P. Miiller[1] and A. Cezairliyan[2]

Received February 26, 1993

A dynamic technique has been used in a microgravity environment to measure the surface tension of tantalum at its melting point. The basic method involves resistively heating a tubular specimen from ambient temperature to temperatures above its melting point in about 1 s by passing an electrical current pulse through it, while simultaneously measuring the pertinent experimental quantities with millisecond resolution. A balance between the magnetic and the surface tension forces acting on the specimen is achieved by splitting the current after it passes through the specimen tube and returning a fraction of the current along the tube axis and the remaining fraction concentrically outside the specimen. Values for surface tension are determined from measurements of the equilibrium dimensions of the molten specimen tube and the magnitudes of the currents. Rapid melting experiments were performed during microgravity simulations with NASA's KC-135 aircraft and the results were analyzed, yielding a value of $2.07 \pm 0.06\ \mathrm{N \cdot m^{-1}}$ for the surface tension of tantalum at its melting point. Conditions for improving specimen stability during temperature excursions into the liquid phase are discussed.

KEY WORDS: dynamic technique; high temperature; melting point; microgravity; surface tension; tantalum.

1. INTRODUCTION

Since the early 1960s, the continuing development of millisecond-resolution dynamic techniques at the National Institute of Standards and Technology (NIST) has enabled the accurate measurement of selected thermophysical properties for a number of electrically conducting refractory solids at high temperatures, primarily in the range 1500 K up to their melting point [1].

[1] Thermophysics Division, National Institute of Standards and Technology, Gaithersburg, Maryland 20899, U.S.A.

[2] Metallurgy Division, National Institute of Standards and Technology, Gaithersburg, Maryland 20899, U.S.A.

0195-928X/93/0900-1063$07.00/0

The techniques involve resistively heating the specimen from room temperature through the temperature range of interest in less than 1 s by passing a large electrical current pulse through it and simultaneously measuring the pertinent experimental quantities with millisecond resolution. Because of the short duration of the heating period (<1 s), the techniques minimize problems associated with specimen evaporation and contamination, large heat transfers, etc., which tend to limit the accuracy of more conventional steady-state techniques, particularly at temperatures above 2000 K. However, millisecond-resolution dynamic techniques are essentially "containerless," and therefore, when used on ground, they are limited to measurements on solids only, since at the melting point, the specimen becomes unstable and collapses due in part to the influence of gravity.

A few years ago, a research effort was undertaken to develop millisecond-resolution dynamic techniques for use in a microgravity environment in order to extend the measurement of thermophysical properties of refractory metals to the liquid phase [2]. As a result of this work, a new dynamic technique for measuring surface tension of liquid metals at high temperatures was developed and its feasibility was successfully demonstrated by performing rapid melting experiments on copper during microgravity simulations with NASA's KC-135 aircraft [3]. The value obtained in these experiments for the surface tension of copper at its melting point was found to be in good agreement with literature data.

The present paper briefly describes the above method for measuring surface tension of liquid metals in a microgravity environment and presents results for the surface tension of tantalum at its melting point, based on microgravity experiments performed during a recent KC-135 flight. In addition, conditions for improving specimen stability during temperature excursions into the liquid phase are discussed. Details regarding the construction and operation of the measurement system, designed for microgravity experiments aboard the KC-135 aircraft, have been given elsewhere [2].

2. METHOD

The basic method consists of resistively heating a tubular specimen in a microgravity environment from ambient temperature to temperatures above its melting point in about 1 s by passing an electrical current pulse through it and, simultaneously, measuring the radiance temperature of the specimen surface by means of a high-speed pyrometer,[3] measuring

[3] The design of the high-speed pyrometer, which operates at a single wavelength of nominally 650 nm, is a modification of that used in the six-wavelength millisecond-resolution pyrometer [4] constructed at NIST.

the electrical currents through and around the specimen, and recording the behavior of the specimen by means of a high-speed framing camera. The specimen is mounted concentrically with respect to the current return paths in a so-called "triaxial" configuration (see below). Static equilibrium of the molten specimen tube is achieved by adjusting the magnitudes of the return currents. Values for surface tension are determined from measurements of the equilibrium dimensions of the molten specimen and the magnitudes of the currents.

A schematic diagram of the triaxial configuration is shown in Fig. 1. In this arrangement, the heating current i, after passing through the specimen tube, is split so that a fraction fi is returned along the axis of the specimen by means of a conducting rod, and the remaining fraction $(1-f)i$ is returned outside the specimen by means of a concentric conducting tube. Because of cylindrical symmetry, the magnetic field generated by the currents has only an azimuthal component B_θ, which will exert an outward pressure proportional to fi at the inside surface of the specimen tube and an inward pressure proportional to $(1-f)i$ on the outside surface. Thus, by a suitable adjustment in the return current split, it should be

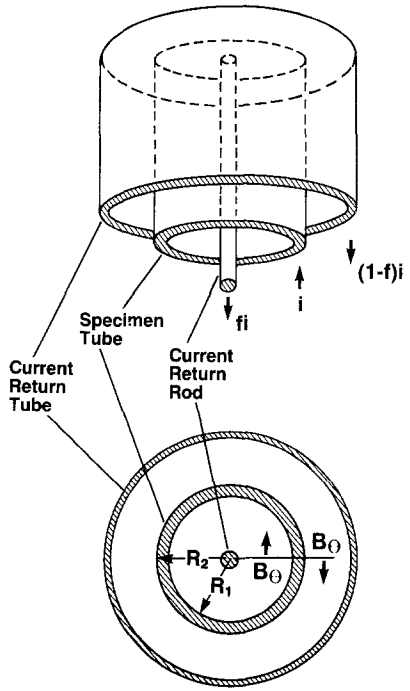

Fig. 1. Schematic diagram of a triaxial configuration for electrical current paths through and around a tubular specimen.

possible to realize a net outward magnetic pressure sufficient to counterbalance the inward pressure of surface tension on the melting specimen. In practice, it is difficult to select a current split that will achieve an exact force balance at the onset of melting. However, results of the present and earlier microgravity experiments have shown that, when (small) imbalances between magnetic and surface tension forces exist at the onset of melting, the melt zone will adjust by expanding or contracting radially until a force balance is achieved and geometrical stability is again reestablished.

A quantitative analysis of the force balance required for static equilibrium within the melt zone of the specimen tube has been given in an earlier publication [3]. It can be shown that if (i) the specimen tube and current return rod are ideally nonmagnetic with magnetic permeability given by $\mu_0 = 4\pi \times 10^{-7}$ H · m, (ii) the pressures exerted by the gas environment at the inner and outer surfaces are equal, and (iii) the melt zone is sufficiently long so there is no axial curvature at the zone midplane during melting, then the surface tension of the molten specimen may be expressed as[4]

$$\gamma = \mu_0 i^2 \frac{R}{2\pi^2(R_2^2 - R_1^2)} \left[\left(\frac{R_1^2}{R_2^2 - R_1^2} + f \right) \ln(R_2/R_1) - \frac{1}{2} \right] \tag{1}$$

where R_1 and R_2 are the respective equilibrium radii of the inner and outer surfaces of the melt zone, and the parameter

$$R = [1/R_2 + 1/R_1]^{-1} \tag{2}$$

The radius of the inside surface, R_1, cannot be observed directly and, so, must be inferred from other measurable quantities.

As mentioned above, the specimen tube will expand or contract radially during melting to accomodate any (small) force imbalance at the onset of melting. Conservation of volume (as required by incompressibility of the liquid) may be satisfied by assuming that the cross-sectional area of the tube remains constant during the radial expansion (or contraction) of the melt zone. Therefore,

$$R_1 = [R_2^2 - t_0(2R_0 - t_0)\alpha]^{1/2} \tag{3}$$

where t_0 and R_0 are the wall thickness and outer surface radius of the tube at the onset of melting, and α is the volume expansion due to melting. Volume rather than areal expansion is used in Eq. (3) since axial expansion of the melt zone is constrained by the solid ends of the specimen tube.

[4] The general case, $0 \leqslant f \leqslant 1$, is considered here for the purpose of discussion in Section 5.2, even though a current split of $f = 1$ was used for all present microgravity experiments on tantalum.

3. MEASUREMENTS

The specimen tubes were cut into 33-mm lengths from 99.9 + % pure tantalum tube stock which had nominal dimensions of 6.35-mm diameter and 0.265-mm wall thickness. The exact wall thickness of each specimen tube was determined from precise measurements of its mass, length, and outside diameter and a literature value ($16.6\,g \cdot cm^{-3}$) for the density of tantalum [5]. Each specimen was mechanically treated with abrasives to remove surface contaminants (oxides, nitrides, etc.) and then stored in an argon environment prior to the KC-135 flight experiments.

The experiment chamber, which provides a triaxial configuration for the specimen, is illustrated schematically in Fig. 2. The specimen tube is clamped between a stationary lower electrode and an upper electrode, which is attached to two flexible (phosphor-bronze) bellows to allow for

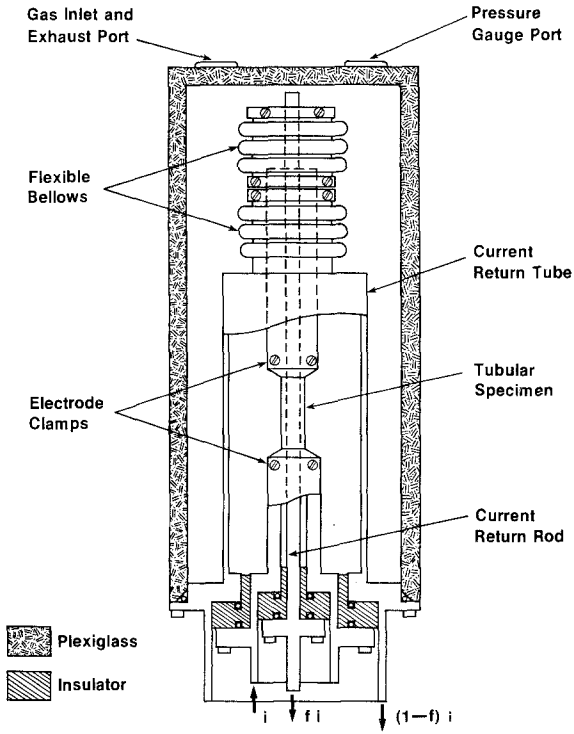

Fig. 2. Schematic diagram of an experiment chamber that enables a tubular specimen to be mounted in a triaxial configuration for rapid melting experiments in a microgravity environment.

thermal expansion of the solid specimen in the axial direction during heating. The specimen is mounted under a small tension at room temperature to approximate the desired condition of zero axial stress during melting. The upper bellows is clamped to a copper rod which enables a fraction of the current fi to be returned along the axis of the specimen. The lower bellows is soldered to a concentric brass tube which permits the remaining fraction of current $(1-f)i$ to be returned outside of the specimen. Axial slots on opposite sides of the brass tube enable the specimen to be viewed by the high-speed pyrometer and the framing camera. The current split is controlled by means of an adjustable resistor (thin-walled Inconel tube) in one of the two current return paths in the pulse-heating system. The magnitude of specimen heating current i is determined by adjustments of a similar resistor in the power-pulsing circuit [2].

In the present microgravity experiments on tantalum, all of the current i passing through the specimen was returned down the copper rod along the axis of the specimen tube, that is, a current split of $f=1$. This eliminated any possible distortion of the melt zone by nonazimuthal magnetic field components that would arise from the axial viewing slots in the brass current return tube. However, in earlier microgravity experiments on copper [3], for which f was in the range 0.77 to 1, such distortions were smaller than other uncertainties involved in determining the molten tube dimensions.

Prior to the KC-135 flight, tantalum tube specimens were mounted in eight identical experiment chambers, which were evacuated and then filled with argon gas at a nominal pressure of 0.1 MPa. The multiple chambers enable the performance of a series of melting experiments during one flight.

During the flight, the aircraft was flown through a series of parabolic maneuvers, each yielding a period of low gravity of about 20 s. In each experiment, the specimen was rapidly heated during the low-g period from ambient temperature through its melting point in less than 1 s by passing an electrical current pulse through it. During heating, the behavior of the specimen was photographed by the framing camera operating at 1000 frames/s, while signals from the high-speed pyrometer, the z-axis accelerometer, and the current measuring devices were recorded every 2 ms by a digital data acquisition system. The pyrometer signal was also displayed on an analog oscilloscope whose image was relayed by means of mirrors through an auxiliary lens in the side of the camera and recorded on the backside of the film. This arrangement greatly facilitated the analysis of the film since frames in which the specimen was melting could be readily identified.

The magnitude of the current during melting in these experiments was in the range 900–950 A. The duration of the heating period in a given

experiment was typically about 0.5 s, which corresponds to a heating rate of about $6000\,\mathrm{K}\cdot\mathrm{s}^{-1}$. The average minimum g level during melting was typically about $1\times10^{-2}\,g$, with a standard deviation of approximately $2\times10^{-2}\,g$. Deviations from the average were due to vibrations transmitted to the specimen mount from the aircraft and from the framing camera.

4. RESULTS

The high-speed photographs recorded during the specimen melting period were analyzed by means of a rear-projection digitizer system to determine the specimen dimensions as a function of time during the melting period. The length of the molten portion of the specimen was approximately $3R_0$, which was sufficient to maintain zero axial curvature of the outside surface near the midplane of the melt zone.

Figure 3 presents a plot of the outer radius R_2 at the melt zone midplane in units of R_0 as a function of elapsed time during the melting period. Each data point represents the average of five successive measurements of the midplane diameter of the melt zone in a given photograph. It may be seen that, after an initial period, the specimen softens and the radius begins to increase in response to an excess outward magnetic pressure until an equilibrium value (dashed line) is reached, indicating a balance between the magnetic and the surface tension forces. The subsequent rapid decrease in radius indicates a premature collapse of the specimen tube that is believed

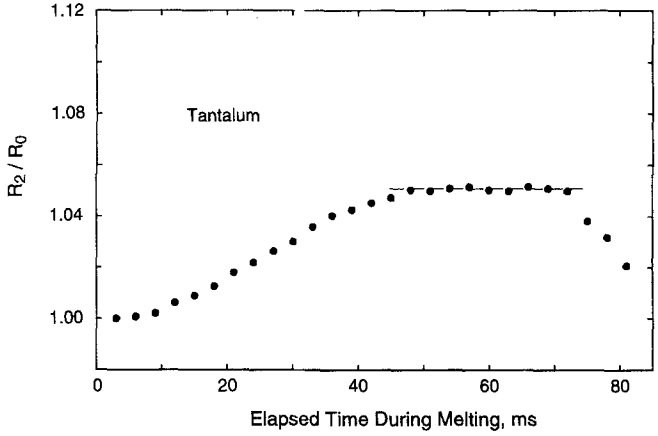

Fig. 3. Variation of the outer surface radius R_2 at the melt zone midplane during rapid melting in a microgravity environment. R_0 is the outer surface radius of the specimen tube just before melting. The dashed line indicates the equilibrium value of the outer surface radius.

Table I. Results on the Determination of Surface Tension of Tantalum at Its Melting Point

Specimen No.	i (A)[a]	R_2/R_0 [b]	$2R_0$ (mm)[c]	t_0 (mm)[c]	γ ($N \cdot m^{-1}$)[d]
1	909	1.051	6.512	0.2726	2.050
2	932	1.092	6.512	0.2719	2.064
3	932	1.084	6.512	0.2714	2.081

[a] Average current passing through the molten specimen tube during the period of static equilibrium.

[b] Average value during the period of static equilibrium.

[c] Specimen tube dimensions at the onset of melting as determined by measurements of outside diameter and wall thickness at room temperature, allowing for linear thermal expansion.

[d] Surface tension of tantalum at its melting point.

to be due to vibration induced instabilities (Section 5.2). In the present microgravity experiments, static equilibrium of the melt zone was successfully achieved for three out of the eight tantalum specimens.

Results for the surface tension of tantalum at its melting point, as obtained from Eqs. (1)–(3), are summarized in Table I. The specimen tube dimensions at the onset of melting, namely, R_0 and t_0, were determined from their measured values at room temperature on the basis of earlier measurements of linear thermal expansion of tantalum performed in our laboratory [6]. Extrapolation of our expansion data to the melting temperature [7] (3257 K on ITS-90) gives 2.55% as the linear expansion of tantalum between room temperature and its melting point. An estimate was used for the volume change due to melting, which, in bcc (body-centered cubic) metals, is approximately 2.5% [8]. The results for the surface tension of tantalum at its melting point were averaged, yielding a mean of 2.065 $N \cdot m^{-1}$, with a standard deviation from the mean of 0.016 $N \cdot m^{-1}$.

The sources of uncertainty[5] in the present measurement of surface tension arise primarily from uncertainties in determining the magnitude of the current and in measuring the outer surface radius of the specimen at both room temperature and during melting. The current passing through the molten specimen during the equilibrium period was determined to within $\pm 1\%$, which corresponds to an uncertainty in surface tension of approximately $\pm 2\%$ or ± 0.04 $N \cdot m^{-1}$. The uncertainty in measuring the outside diameter of each specimen tube at room temperature is estimated to be no greater than $\pm 0.5\%$, which corresponds to an uncertainty in the

[5] Magnitudes expressed as either an estimated maximum uncertainty or an expanded uncertainty. Expanded uncertainty is determined by multiplying the standard uncertainty (estimated standard deviation) by a coverage factor whose value, by convention, is equal to 2.

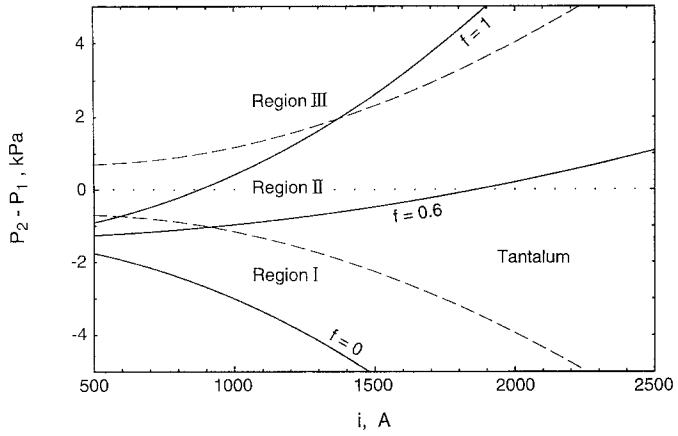

Fig. 4. Differences in gas pressure at the inner (P_1) and outer (P_2) surfaces, that are required to balance magnetic and surface tension forces so that $R_2/R_0 = 1$ during melting, as a function of current passing through the specimen tube at values for the return current split f between 0 and 1 (solid curves). The dashed curves define regions of specimen stability with respect to surface perturbations, as described in the text.

value of surface tension of $\pm 0.01\ \mathrm{N \cdot m^{-1}}$. The ratios R_2/R_0 were determined to within $\pm 1\%$ from measurements on the high-speed photographs, thereby contributing an additional uncertainty in surface tension of $\pm 0.03\ \mathrm{N \cdot m^{-1}}$. Other sources of uncertainty, such as uncertainties arising from the use of literature values for density of tantalum at room temperature [5], linear thermal expansion of solid tantalum at high temperatures [6], and volume change of tantalum due to melting [8], each contribute a small uncertainty to the value of surface tension of not greater than $0.001\ \mathrm{N \cdot m^{-1}}$. Thus, the total uncertainty in the present measurement of surface tension is taken as the square root of the sum of squares of the individual uncertainties (rounded upward), yielding $\pm 0.06\ \mathrm{N \cdot m^{-1}}$.

Therefore, on the basis of the present measurements, it is concluded that the surface tension of tantalum at its melting point is $2.07\ \mathrm{N \cdot m^{-1}}$, with an uncertainty of $\pm 0.06\ \mathrm{N \cdot m^{-1}}$.

5. DISCUSSION

5.1. Surface Tension of Tantalum at Its Melting Point

In view of the high reactivity of liquid refractory metals, it is not surprising to find relatively few measurements of the surface tension of

tantalum at its melting point reported in the literature. A comparison of the present result with other literature data is given in Table II.

The earlier data were obtained by one of two techniques, either the pendant-drop method or the drop-weight method. Both are quasi-steady-state methods that require an accurate knowledge of density and shape (pendant-drop) or size (drop-weight) of a suspended liquid drop and involve a balance between the surface tension and the force of gravity [9]. In contrast, the present dynamic technique requires accurate dimensional knowledge of the molten tube in the absence of gravity and involves a balance between surface tension and magnetic forces.

The value for the surface tension of tantalum at its melting point reported by Allen [9], namely, $2.15\ N \cdot m^{-1}$, was based on measurements with both pendant-drop and drop-weight methods and a liquid density ($15.0\ g \cdot cm^{-1}$) calculated from literature data on room temperature density, cubical thermal expansion, and volume change due to melting. This value is about 4% higher than the present result of $2.07\ N \cdot m^{-1}$, a difference that is within experimental uncertainties. More recently, Eremenko et al. [10] used the pendant-drop method to obtain a value of $2.016\ N \cdot m^{-1}$, based on their measurement of liquid density ($14.13\ g \cdot cm^{-1}$) with a drop-weight technique. Their reported value for surface tension is about 3% lower than the present result.

The apparently large difference between results for surface tension reported by Allen and by Eremenko et al. is almost entirely due to different values used for the density of liquid tantalum. In fact, the liquid density measured by Eremenko et al. appears to be somewhat low since, based on our recent accurate measurements of thermal expansion of tantalum up to near its melting point [6], their value would require the volume change due to melting to be about 9% in order to account for the total change in

Table II. Values for the Surface Tension of Tantalum at Its Melting Point Reported in the Literature

Investigator(s)	Ref. No.	Year	Technique[a]	Liquid density ($g \cdot cm^{-3}$)	Surface tension ($N \cdot m^{-1}$)
Allen	9	1963	PD, DW	15.0[b]	2.15 ± 0.04
Eremenko et al.	10	1984	PD	14.13[c]	2.016
Present work			DM		2.07 ± 0.06

[a] Method used to measure surface tension: PD, pendant-drop method; DW, drop-weight method; DM, dynamic technique in microgravity.

[b] Calculated by the investigator on the basis of literature data for density at room temperature, linear thermal expansion up to m.p., and volume change due to melting.

[c] Measured by the investigators using a drop-weight method.

density from its room temperature value [5]. Reported values of volume change due to melting for bcc metals are typically in the range 1.7 to 3.5% [8].

Because of the sensitivity of surface tension to surface contaminants (nitrides, oxides, etc.), surfaces of the specimen tubes were mechanically abraded prior to use in the present microgravity experiments. Such treatments have proven effective in removing preexisting surface contaminants in earlier dynamic measurements on another surface-sensitive property, namely, the surface radiance temperature of a metal at its melting point [11]. These earlier measurements, which were performed on a number of refractory metals including tantalum, also indicated that there is minimal surface contamination by the argon gas environment during subsecond-duration pulse heating experiments.

5.2. Specimen Stability in a Triaxial Configuration

In the present measurements on tantalum, as in earlier microgravity experiments on copper [3], the thin-walled tubular specimens tended to collapse during melting prior to any significant excursion into the liquid phase. A possible explanation suggested in the earlier study is that instabilities, generated by perturbations of the specimen inner and outer surfaces (as a result of vibrations transmitted to the experiment chamber), may be responsible for this behavior.

The effect of axisymmetric surface perturbations on the stability of an infinitely long current-carrying liquid tube, mounted in a triaxial configuration under gravity-free conditions, has been the subject of a theoretical investigation by MacDonald [12]. Dispersion relations were obtained for the two normal modes of vibration, one in which the inner and outer surfaces move in phase and the other in which the relative surface movements are out of phase. When applied to the actual experimental condition of equal gas pressures inside and outside the tube, the results indicated that the in-phase modes are always stable, but the out-of-phase modes are unstable for long-wavelength vibrations. Thus, the premature collapse of specimen tubes in our microgravity experiments appears to be due to the presence of long-wavelength out-of-phase modes of vibration.

Recently, the above theoretical study was extended to include the case of unequal gas pressures inside (P_1) and outside (P_2) the tube [13]. The results are presented in Fig. 4, where the gas pressure difference $P_2 - P_1$ needed to balance the magnetic and surface tension forces such that $R_2/R_0 = 1$ is plotted as a function of current passing through the specimen for values of current split f between 0 and 1 (solid curves). The dashed curves define three distinct regions of specimen stability: Region I, the

in-phase and out-of-phase modes are unstable for vibrations at all wavelengths; Region II, the in-phase modes are always stable but the out-of-phase modes are unstable for long-wavelength vibrations; and Region III, both in-phase and out-of-phase modes are always stable. This suggests that molten specimen tubes will remain stable in microgravity experiments with $f = 1$ as long as suitable values for i (> 1400 A) and $P_2 - P_1$ (> 2 kPa) are used to maintain a balance among magnetic, surface tension, and gas pressure forces.

The effect of nonaxisymmetric perturbations on specimen stability was not considered in the above study. However, Chow and Harvanek [14] have reported on a more general stability analysis of a current-carrying liquid tube, but without a current return rod (equivalent to $f = 0$ in the present case). Their analysis shows that, in the absence of a current, the liquid tube is stable with respect to all nonaxisymmetric perturbations. Furthermore, they suggest that such perturbations are likely to be more stable than axisymmetric ones when a current is present.

6. CONCLUDING REMARKS

A dynamic method for measuring surface tension of liquid metals in a microgravity environment has been used to determine the surface tension of tantalum at its melting point. The results are in good agreement with the limited amount of data available in the literature, which are based on quasi-steady-state measurements performed on ground. The short duration of the experiment (< 1 s) in the present work makes our dynamic technique particularly suited to measuring the surface tension of liquid refractory metals because of their high reactivity and the sensitivity of their surface tension to contaminants.

In order to avoid premature collapse of the molten specimen tube in future microgravity experiments, a redesign of the experiment chamber will be required to maintain and control a gas pressure difference between the inside and the outside of the specimen tube. In this way, significant temperature excursions into the liquid phase should be possible, which will enable the determination of the temperature coefficient of surface tension, as well as other thermophysical properties such as heat of fusion and heat capacity and electrical resistivity of the liquid specimen.

ACKNOWLEDGMENTS

This work was supported by the Microgravity Science and Applications Division of NASA. The authors gratefully acknowledge the assistance of J. Welch of NIST/Boulder, R. Shurney of NASA/MSFC, and R. Williams

of NASA/JSC during the preparations for and the performance of the microgravity experiments. The authors are particularly grateful to R. A. MacDonald of NIST/Gaithersburg for helpful discussions and for providing the numerical computations in relation to specimen stability.

REFERENCES

1. A. Cezairliyan, *Int. J. Thermophys.* **5**:177 (1984).
2. A. Cezairliyan and A. P. Miiller, *Int. J. Thermophys.* **11**:653 (1990).
3. A. P. Miiller and A. Cezairliyan, *Int. J. Thermophys.* **11**:663 (1990).
4. A. Cezairliyan, G. M. Foley, M. S. Morse, and A. P. Miiller, in *Temperature: Its Measurement and Control in Science and Industry, Vol. 6, Part 2*, J. F. Schooley, ed. (AIP, New York, 1992), p. 757.
5. T. E. Tietz and J. W. Wilson, *Behavior and Properties of Refractory Metals* (Stanford University Press, CA, 1965), p. 28.
6. A. P. Miiller and A. Cezairliyan, *Int. J. Thermophys.* **3**:259 (1982).
7. L. Malter and D. B. Langmuir, *Phys. Rev.* **55**:743 (1939).
8. R. N. Lyon, *Liquid Metals Handbook*, 2nd ed. (rev.) (AEC and U.S. Navy, Washington, DC, 1954).
9. B. C. Allen, *Trans. Metallurg. Soc. AIME* **227**:1175 (1963).
10. V. N. Eremenko, Yu. N. Ivashenko, and P. S. Martensyuk, *High Temp. (USSR)* **22**:567 (1984).
11. A. Cezairliyan, A. P. Miiller, F. Righini, and A. Rosso, in *Temperature: Its Measurement and Control in Science and Industry, Vol. 6, Part 1*, J. F. Schooley, ed. (AIP, New York, 1992), p. 377.
12. R. A. MacDonald, *J. Appl. Phys.* **66**:5302 (1989).
13. R. A. MacDonald, private communication.
14. C.-Y. Chow and M. Harvanek, in *Proceedings of the 1st National Fluid Dynamics Congress* (American Institute of Aeronautics and Astronautics, New York, 1988), Part 3, p. 1805.